MedChemComm

RESEARCH ARTICLE

View Article Online
View Journal | View Issue

Cite this: *Med. Chem. Commun.*, 2018, **9**, 1871

Selected aryl thiosemicarbazones as a new class of multi-targeted monoamine oxidase inhibitors†

Bijo Mathew, ‡*[a] Seung Cheol Baek,‡[b] Della Grace Thomas Parambi,[c] Jae Pil Lee,[b] Monu Joy,[d] P. R. Annie Rilda,[a] Rugma V. Randev,[a] P. Nithyamol,[a] Vijitha Vijayan,[a] Sini T. Inasu,[a] Githa Elizabeth Mathew,[e] Krishnakumar K. Lohidakshan,[f] Girish Kumar Krishnan[g] and Hoon Kim*[b]

Received 14th August 2018,
Accepted 23rd September 2018

DOI: 10.1039/c8md00399h

rsc.li/medchemcomm

A series of 13 phenyl substituted thiosemicarbazones (**SB1**–**SB13**) were synthesized and evaluated for their inhibitory potential towards human recombinant monoamine oxidase A and B (MAO-A and MAO-B, respectively) and acetylcholinesterase. The solid state structure of **SB4** was ascertained by the single X-ray diffraction technique. Compounds **SB5** and **SB11** were potent for MAO-A (IC_{50} 1.82 ± 0.14) and MAO-B (IC_{50} 0.27 ± 0.015 μM), respectively. Furthermore, **SB11** showed a high selectivity index (SI > 37.0) for MAO-B. The effects of fluorine orientation revealed that **SB11** (*m*-fluorine) showed 28.2 times higher inhibitory activity than **SB12** (*o*-fluorine) against MAO-B. Furthermore, inhibitions by **SB5** and **SB11** against MAO-A and MAO-B, respectively, were recovered to near reference levels in reversibility experiments. Both **SB5** and **SB11** showed competitive inhibition modes, with K_i values of 0.97 ± 0.042 and 0.12 ± 0.006 μM, respectively. These results indicate that **SB5** and **SB11** are selective, reversible and competitive inhibitors of MAO-A and MAO-B, respectively. Compounds **SB5**, **SB7** and **SB11** showed moderate inhibition against acetylcholinesterase with IC_{50} values of 35.35 ± 0.47, 15.61 ± 0.057 and 26.61 ± 0.338 μM, respectively. Blood–brain barrier (BBB) permeation was studied using the parallel artificial membrane permeation assay (PAMPA) method. Molecular docking studies were carried out using AutoDock 4.2.

Introduction

The role of monoamine oxidases (MAOs) in brain neurochemistry is mainly connected with the oxidative deamination of biogenic amines (BA).[1] Amines such as adrenaline, noradrenaline, melatonin and serotonin are predominantly metabolized by MAO-A, whereas benzylamine and phenylethylamine are controlled by MAO-B. Both types of MAO isoforms have common substrates such as dopamine and tyramine.[2,3] Selective MAO inhibitors (MAOIs) have a great impact on treating various psychiatric and neurodegenerative disorders by depleting MAO levels in the brain.[4] Serotonin, the concentration of which is maintained by inhibitors of MAO-A, shows superior antidepressant activity.[5] Conversely, the end-products, hydrogen peroxide and reactive oxygen species (ROS), produced during dopamine metabolism by MAO-B, generate oxidative stress and apoptosis in dopamine producing cells. These highly reactive toxic radicals produce neural toxicity which may be the prime indications for Alzheimer's and Parkinson's diseases (AD & PD).[6] Hence, selective MAO-B inhibitors are highly recommended as co-adjuvant therapy for treating AD and PD patients.[7,8]

The current scenario of PD therapy focuses on restoring the level of dopamine in the brain and thereby curtailing the motor symptoms.[9] This therapy is accelerated by the administration of dopamine precursors (L-DOPA), dopamine agonists, catechol-*O*-methyltransferase (COMT) and MAO-B inhibitors such as selegiline and rasagiline (highly selective and irreversible).[10] Molecules which have closer acetylcholinesterase (AChE) and MAO-B affinities are able to limit the neurotoxicity related to sources of ROS in age-related AD

[a] *Division of Drug Design and Medicinal Chemistry Research Lab, Department of Pharmaceutical Chemistry, Ahalia School of Pharmacy, Palakkad-678557, Kerala, India. E-mail: bijovilaventgu@gmail.com*
[b] *Department of Pharmacy and Research Institute of Life Pharmaceutical Sciences, Sunchon National University, Suncheon-57922, Republic of Korea. E-mail: hoon@sunchon.ac.kr*
[c] *Department of Pharmaceutical Chemistry, Jouf University, Al Jouf-2014, Sakaka, Saudi Arabia*
[d] *School of Pure & Applied Physics, M.G. University, Kottayam, Kerala, India*
[e] *Department of Pharmacology, Grace College of Pharmacy, Palakkad, India*
[f] *Department of Pharmaceutical Chemistry, Nirmala College of Health Science, Chalakudy-680311, India*
[g] *Department of Pharmaceutical Chemistry, College of Pharmaceutical Sciences, Government Medical College Trivandrum, India*

† Electronic supplementary information (ESI) available. CCDC 1852751. For ESI and crystallographic data in CIF or other electronic format see DOI: 10.1039/c8md00399h

‡ These authors contributed equally.

diseases.[11] In 2011, the molecule ladostigil, a dual inhibitor of both AChE and MAO-B designed by Youdim, entered into the phase II clinical trial for the treatment of AD.[12] Considering the complex pathogenetic factors of various neurodegenerative diseases, it is highly appropriate to recommend selective MAO-B inhibitors with cocktail therapy to trigger the multi-targets associated with these diseases.

The MAO-B inhibitors currently in use are the irreversible type, having a covalent bond to the FAD unit of the inhibitor binding cavity (IBC) of the enzyme.[13] Disruption of the target, a poor ADME profile and increased duration of action occur due to this irreversible binding. Hence, the development of reversible MAO-B inhibitors has a greater therapeutic value in treating neurodegenerative diseases.[14] Some of the evidence also documents that mild symptomatic benefits were gained *via* the administration of moclobemide (a reversible MAO-A inhibitor) when combined with levodopa for the treatment of PD.[15,16] Recently, many small molecules like chalcones, coumarins and chromones have shown considerable potential for the development of MAO-A/MAO-B inhibitors with a highly selective and reversible mode of inhibition.[17–19]

From a chemical point of view, thiosemicarbazones are thiourea compounds linked with an azomethine scaffold and are the key intermediates for the synthesis of 2-amino-1,3,4-thiadiazoles *via* a ring chain tautomerism mechanism.[20,21] Besides this, thiosemicarbazones are excellent chelators of transition metals such as zinc (Zn), copper (Cu) and iron (Fe), which are potent inhibitors of various carcinogenesis-inducing pathways.[22] In the past, many efforts have addressed the development of thiosemicarbazone-based MAOIs.[23–29] Moreover, the cyclized form of thiosemicarbazones from chalcones afforded *N*-thiocarbamoyl pyrazolines, which show a remarkable inhibition profile against MAOs.[30–34] The presence of hydrazine units in thiosemicarbazide also afforded a number of hydrazone scaffolds *via* the acid catalyzed nucleophilic addition mechanism.[35] Numerous studies recommend the multi-potent MAO and cholinesterase inhibitors for treating AD and PD.[36,37] Accordingly, this work describes the synthesis of phenyl-substituted thiosemicarbazones, the studies on MAO and acetylcholinesterase inhibition, and the kinetics of the inhibition mechanism of MAOs using Lineweaver–Burk plots, the reversibility mode, and blood–brain barrier (BBB) permeation assays. Finally, the lead molecules from the *in vitro* results were subjected to molecular docking studies to elucidate the binding interactions of both MAO-A and B.

Result and discussion

Chemistry

The target aryl thiosemicarbazones were synthesized as presented in Scheme 1. Synthesis was accomplished by the single step reaction between commercially available thiosemicarbazide hydrochloride and various substituted benzaldehydes. In the ^{1}H-NMR spectra, the sharp singlet peak observed between 7.71–7.89 is ascribed to the azomethine (–CH=N–) proton. The downfield proton of the NH group attached to the thiocarbamoyl unit is observed in the range between 9.18–9.88. Two broad singlets were found at 6.23–7.25 and 7.23–7.26, corresponding to the terminal NH_2 group. ^{13}C NMR spectra displayed carbothioamide groups for **SB1–SB13** between δ180.60–184.30. All spectral characterization results are in full agreement with previous literature reports.[38–40] The solid state structure of **SB4** was ascertained by the single X-ray diffraction technique, and the ORTEP diagram is depicted in Fig. 1. The mass spectra of all fluorinated chalcones showed intensive molecular ions, assisting the structure of the targeted compounds.

Monoamine oxidase inhibition studies

Inhibition profile of aryl substituted thiosemicarbazones. Six different compounds of the derivatives showed high inhibitory activities (more than 50%) against MAO-A or MAO-B, while the other compounds were not effective (Table 1).

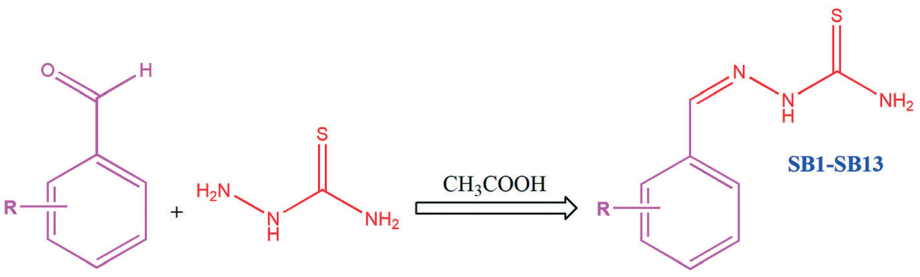

R		R	
SB1	:H	SB8	:4-Cl
SB2	:4-OH	SB9	:4-Br
SB3	:4-OCH_3	SB10	:4-F
SB4	:4-CH_3	SB11	:3-F
SB5	:4-$N(CH_3)_2$	SB12	:2-F
SB6	:4-C_2H_5	SB13	:4-CF_3
SB7	:4-NO_2		

Scheme 1 Synthetic route of aryl thiosemicarbazones.

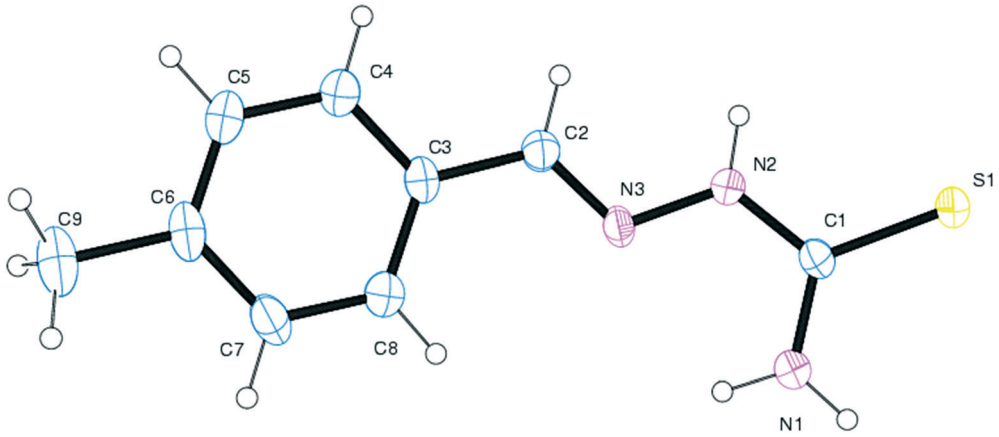

Fig. 1 ORTEP diagram of compound **SB4**.

Table 1 Inhibition of recombinant human MAO enzymes and acetylcholinesterase by aryl substituted aryl thiosemicarbazones[a]

	Residual activity at 10 μM (%)		IC_{50} (μM)			
Compounds	MAO-A	MAO-B	MAO-A	MAO-B	AChE	SI[b]
SB1	83.5 ± 0.7	75.5 ± 0.7	>10.0	>10.0	>40.0	—
SB2	66.0 ± 1.4	87.5 ± 3.5	>10.0	>10.0	>40.0	—
SB3	37.5 ± 0.7	82.1 ±1.4	4.99 ± 0.25	>10.0	36.14 ± 0.45	<0.50
SB4	56.5 ± 0.7	91.5 ± 2.1	>10.0	>10.0	>40.0	—
SB5	16.5 ± 2.1	82.3 ± 1.4	1.82 ± 0.14	>10.0	35.35 ± 0.47	<0.18
SB6	36.0 ± 5.7	86.2 ± 1.4	5.98 ± 0.15	>10.0	26.72 ± 0.006	<0.60
SB7	75.5 ± 3.5	7.5 ± 0.7	>10.0	1.43 ± 0.014	15.61 ± 0.057	>6.99
SB8	76.0 ± 1.4	60.5 ± 2.1	>10.0	>10.0	>40.0	—
SB9	59.5 ± 0.7	82.5 ± 4.9	>10.0	>10.0	31.12 ± 0.44	—
SB10	84.5 ± 3.5	86.5 ± 2.1	>10.0	>10.0	37.93 ± 0.57	—
SB11	75.5 ± 2.1	3.0 ± 1.4	>10.0	0.27 ± 0.015	26.61 ± 0.34	>37.0
SB12	77.5 ± 0.7	33.5 ± 2.1	>10.0	7.61 ± 0.49	30.84 ± 0.58	>1.31
SB13	92.5 ± 0.7	77.5 ± 0.7	>10.0	>10.0	36.23 ± 0.44	—
Toloxatone	—	—	0.92 ± 0.016	>80	—	<0.012
Lazabemide	—	—	>80	0.042 ± 0.0010	—	>1900
Clorgyline	—	—	0.0071 ± 0.0003	1.69 ± 0.32	—	0.0042
Pargyline	—	—	1.31 ± 0.068	0.091 ± 0.005	—	14.4
Tacrine	—	—	—	—	0.23 ± 0.014	—

[a] Results are expressed as means ± standard errors of duplicate experiments. Inhibitory activities for reference compounds of MAO and AChE were measured after preincubation with the enzymes for 30 min and 15 min, respectively. [b] SI was expressed for MAO-B by dividing the IC_{50} value of MAO-A by that of MAO-B.

Compounds **SB3**, **SB5**, and **SB6** showed efficient inhibition against MAO-A with IC_{50} values of 4.99 ± 0.25, 1.82 ± 0.14, and 5.98 ± 0.15 μM, respectively. Compounds **SB7**, **SB11**, and **SB12** were also effectively inhibitory against MAO-B with IC_{50} values of 1.43 ± 0.014, 0.27 ± 0.015, and 7.61 ± 0.49 μM, respectively. All 6 compounds showed good selectivity, and **SB5** and **SB11** were the most potent for MAO-A and MAO-B, respectively. Furthermore, **SB11** showed a high selectivity index (SI > 37.0) for MAO-B with a low IC_{50} value (0.27 μM), suggesting it is a good candidate for selective MAO-B inhibition. Considering the structural comparisons, we concluded that based on their IC_{50} values, the *m*-fluorine substitution of the compounds (**SB11**) showed 28.2 times higher inhibitory activity against MAO-B than *o*-fluorine substitution (**SB12**) and >37.0 times more potent than *p*-fluorine (**SB10**) (Table 1). However, the substituent *p*-NO_2 (**SB7**) was more effective than the *p*-fluorine substituent (**SB10**).

The potency of **SB5** for MAO-A (IC_{50} = 1.82 μM) was lower than that of **IM5** (IC_{50} = 0.30 μM), which is a synthesized imidazole-bearing chalcone derivative of the eleven series and is the most potent for MAO-A reported by our group recently.[41] However, the SI value of **SB5** (0.18) in this study was >4.2 times greater than that of **IM5** (0.75). The potency of **SB11** for MAO-B (IC_{50} = 0.27 μM) was higher than that of **IM4** (IC_{50} = 0.32 μM), which is another derivative and the most potent for MAO-B in the **IM** series. Similar to **SB5**, the SI value of **SB11** (>37.0) was >11.2 times higher than that of **IM4** (3.3). Although the potency of **SB11** for MAO-B was 6.4 times lower than that of the marketed drug lazabemide for MAO-B (IC_{50} = 0.042 μM), the relatively low molecular weight

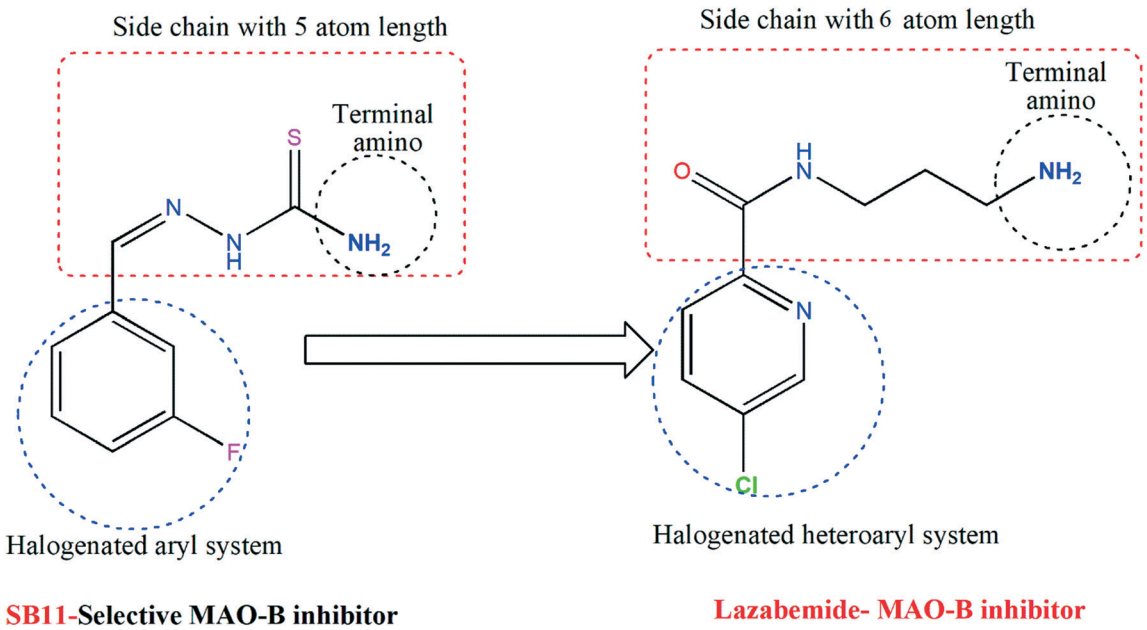

Fig. 2 Similarity-based structures of **SB11** and a standard MAO-B inhibitor.

of **SB11** (MW = 197.2) is comparable to that of lazabemide (MW = 199.6) and lower than that of **IM4** (MW = 288.3); it also has an IC_{50} value comparable to that of lazabemide in the nanomolar concentration range. The structural features

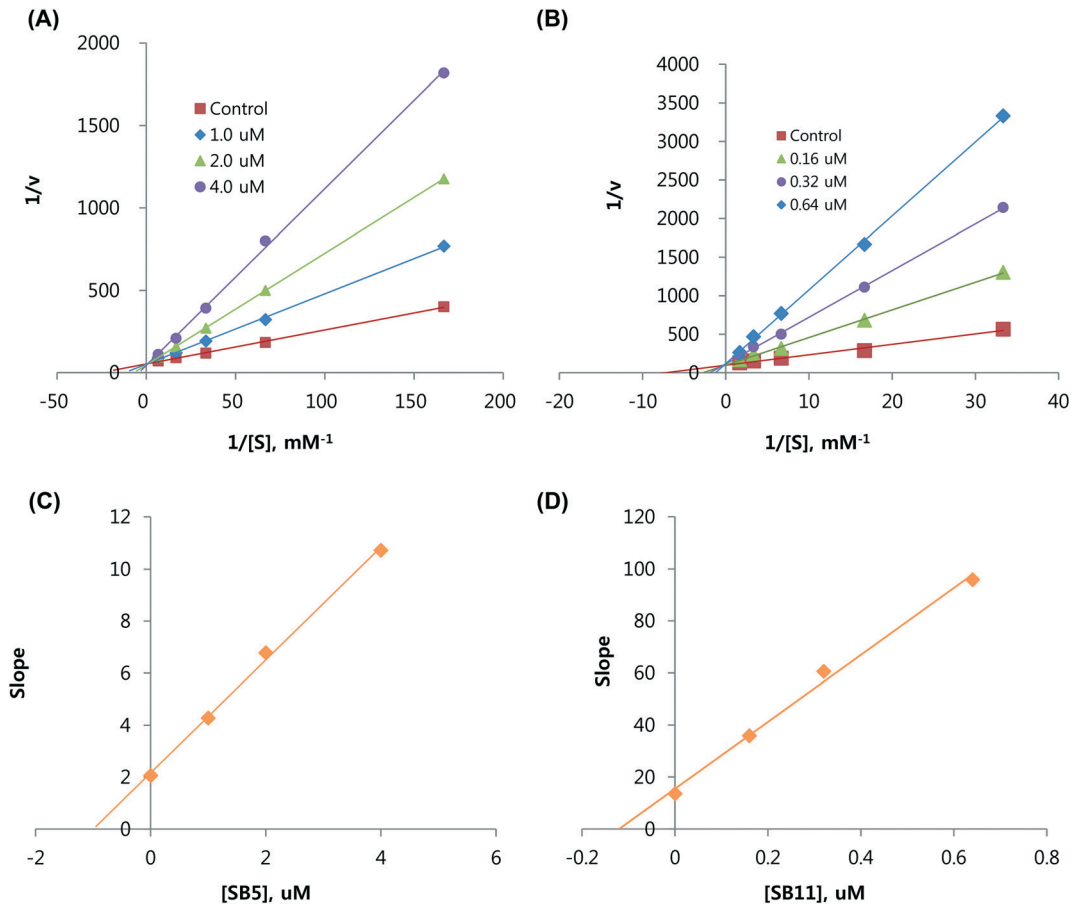

Fig. 3 Kinetic analyses of inhibition of MAO-A by **SB5** (A) and of MAO-B by **SB11** (C) using Lineweaver–Burk plots, and their respective secondary plots of slopes *vs.* inhibitor concentrations of **SB5** (B) and **SB11** (D).

of **SB11** were mainly divided as follows: (a) a halogenated aryl system, (b) a side chains with an almost similar length to that of lazabemide, and (c) a terminal amino group at the side chain. Similar types of features are seen in the potent MAO-B inhibitor (lazabemide) and these are depicted in Fig. 2. These structural features are responsible for the design and development of a new class of MAO-B inhibitors.

Structure–activity relationship (SAR) analysis of MAO inhibition. Changes in the MAO inhibitory potency of the tested aryl thiosemicarbazones could be correlated to the effect of various electron donating and withdrawing groups anchored to the phenyl system. To explore the structure–activity relationship of the target compounds, we initially focused on varying the substituents at the *para* position of the phenyl system of aryl thiosemicarbazones. Unsubstituted aryl thiosemicarbazones are less effective against both MAO-A and MAO-B with $IC_{50} > 10.0$ μM. Modifications in the position and orientation of substituents on the phenyl system result in a shift in this trend. The presence of electron donating groups (EDGs) such as methoxy, dimethylamino and ethyl on the *para* position of the phenyl system in compounds **SB3**, **SB5** and **SB6** significantly contributes to the activity ratio towards MAO-A. Furthermore, introduction of electron donating groups such as hydroxyl and methyl (**SB2** & **SB4**) results in a dramatic decrease in activity. Hence, it is commonly recommended that EDGs with bulky groups on the phenyl system of aryl thiosemicarbazones adapt well in the hydrophobic pocket of the inhibitor binding cavity (IBC) of MAO-A. Shifting of MAO-A selectivity was revealed after the introduction of an electron withdrawing nitro group. The presence of halogens such as chlorine, bromine and fluorine at the *para* position of aryl thiosemicarbazones had no impact on MAO-B inhibition. In particular, shifting of the fluorine atom to the *meta* position results in more potent MAO-B inhibition (**SB11**) with a *K*i value of 0.12 ± 0.006 μM. This inhibition constant value was found to be better than that of the standard hMAO-B inhibitor (irreversible type) which was reported previously by our research group.[42–50]

Kinetics. The inhibition modes of **SB5** and **SB11** for MAO-A and MAO-B, respectively, were analyzed using Lineweaver–Burk plots. The plots for **SB5** and **SB11** were linear and intersected the *y*-axis (Fig. 3A and C). The K_i values determined from the secondary plot (the slopes of the Lineweaver–Burk plots *vs.* the inhibitor concentrations) of MAO-A inhibition by **SB5** and MAO-B inhibition by **SB11** were 0.97 ± 0.042 and 0.12 ± 0.006 μM, respectively (Table 1, Fig. 3B and D). These results indicate that **SB5** and **SB11** are selective and reversible competitive inhibitors of MAO-A and MAO-B, respectively.

Reversibility studies. No changes in the residual activities were observed when **SB5** and **SB11** were preincubated with MAO-A and MAO-B, respectively, for up to 30 min. In the reversibility experiments, the A_U and A_D values obtained using **SB5** for MAO-A were 34.7% and 70.3%, respectively (Fig. 4A). The values for toloxatone (a reversible inhibitor) reference experiments for MAO-A were 30.7% and 74.0%, respectively, and the values for clorgyline (an irreversible inhibitor) were

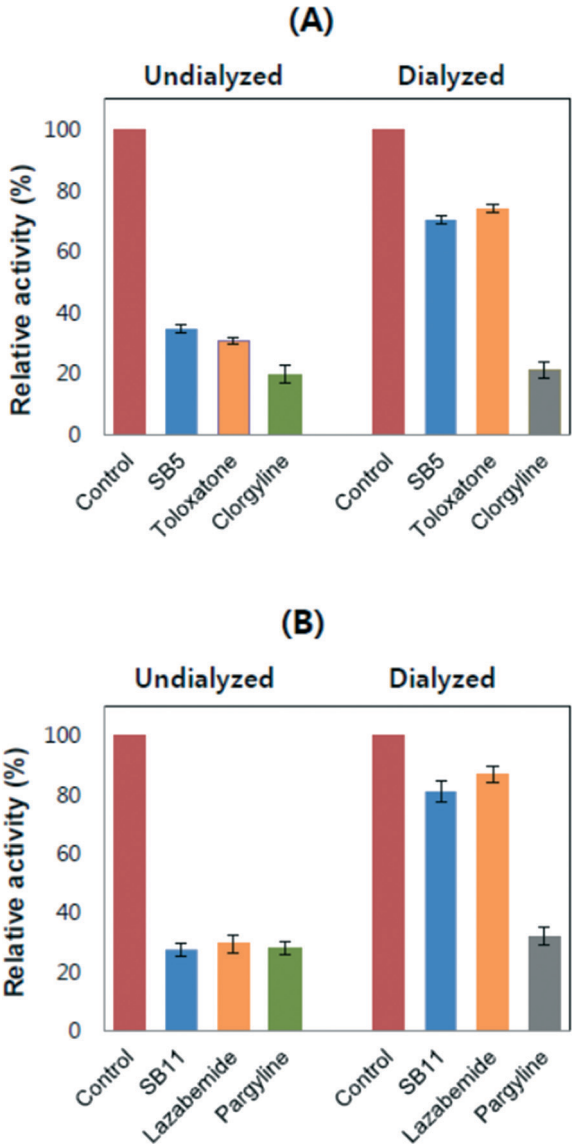

Fig. 4 Reversibility of MAO enzymes by aryl substituted thiosemicarbazones. MAO-A and MAO-B were inhibited at approximately 2 × IC_{50} by **SB5** (A) and **SB11** (B), respectively, and the activities were recovered by dialysis experiments against 100 mM sodium phosphate (pH 7.2) before measuring the residual activities. Concentrations of inhibitors and references used: **SB5**, 3.6 μM; toloxatone, 2.0 μM; clorgyline, 0.014 μM; **SB11**, 0.54 μM; lazabemide, 0.08 μM; pargyline, 0.20 μM.

21.4% and 19.8%, respectively. The inhibition by toloxatone was greatly recovered by dialysis, while inhibition by clorgyline was not recovered. Similar to these results, the activity by **SB5** was recovered close to the reversible reference level. The enzymatic activity of MAO-B by **SB11** revealed A_U and A_D values of 27.4% and 81.0%, respectively (Fig. 4B); the values for lazabemide were 29.5% and 86.9%, respectively, and those for pargyline were 27.9% and 32.0%, respectively. MAO-B inhibition by pargyline was not recovered by dialysis, whereas the activity by lazabemide was greatly recovered, similar to the recovery to near reference levels of the inhibitory activity by **SB11**. These results indicate that analogues

Table 2 Results of PAMPA-BBB assay of aryl thiosemicarbazones and commercial drugs

Compounds[a]	Bibliography Pe[b] ($\times 10^{-6}$ cms^{-1})	Experimental Pe[c] ($\times 10^{-6}$ cms^{-1})	Prediction
SB3	—	11.24 ± 0.44	CNS+
SB5	—	10.14 ± 0.56	CNS+
SB6	—	09.44 ± 0.65	CNS+
SB7	—	12.78 ± 0.45	CNS+
SB11	—	13.12 ± 0.54	CNS+
SB12	—	10.33 ± 0.22	CNS+
Testosterone	17.0	17.33 ± 0.12	CNS+
Progesterone	9.3	08.13 ± 0.42	CNS+
Dopamine	0.2	0.21 ± 0.01	CNS−
Hydrocortisone	1.8	1.71 ± 0.02	CNS−

[a] Compounds were dissolved in DMSO to a concentration of 5 mg mL^{-1} and diluted with PBS/EtOH (70 : 30). The final concentration of the compound was 100 μg mL^{-1}. [b] Taken from ref. 51. [c] Values are expressed as the mean ± SEM of three independent experiments.

SB5 and **SB11** are reversible inhibitors of MAO-A and MAO-B, respectively.

Acetylcholinesterase inhibition

As presented in Table 1, it was noted that all the compounds are moderate and less potent than the reference compound tacrine for AChE inhibition. Considering the type of substitution at the phenyl ring, the inhibitory potency against AChE clearly favored the electron withdrawing nitro group at the *para* position of the phenyl system (**SB7**, IC_{50} 15.61 ± 0.057 μM). According to the data, the presence of a chlorine or hydroxyl group is not crucial for imparting inhibitory potential against AChE in aryl thiosemicarbazones. All the fluorinated thiosemicarbazones showed moderate AChE inhibition. The *ortho*- and *meta*-substituted analogues **SB12** and **SB11** show slightly higher AChE inhibitory activities compared to the *para*-substituted analogue **SB10**, likely being MAO-B inhibition.

Blood–brain barrier (BBB) permeation assay

An essential requirement for successful CNS drugs is the ability to cross the BBB, which is determined using the parallel artificial membrane permeation assay (PAMPA). According to the limits established by Di *et al.*, BBB permeation test compounds are classified as follows:[51]

CNS + (high BB permeation predicted) : Pe($\times 10^{-6}$ cms^{-1}) − >4.00

CNS − (high BB permeation predicted) : Pe($\times 10^{-6}$ cms^{-1}) − >2.00

Table 2 shows the permeability results of the PAMPA-BBB assay of commercial drugs and the 6 top ranked aryl thiosemicarbazones. Our results indicate that all the tested thiosemicarbazones are capable of crossing the BBB to target the MAO-A and MAO-B enzymes in the central nervous system (CNS), which is consistent with our design strategy.

Molecular docking

From the *in vitro* results, it is evident that compounds **SB5** and **SB11** show a good inhibitory profile towards MAO-A and MAO-B, respectively, in the micro molar range. We therefore attempted to investigate the hypothetical binding modes of the respective compounds in the IBC of isoenzymes. Of the 50 runs in the docking methodology, we selected the highest binding energy in the largest cluster for the hypothetical binding pose. The binding mode of **SB5** (an hMAO-A inhibitor) is shown in Fig. 5. The presence of imino nitrogen and a terminal amino group in **SB5** contributes significant hydrogen bonding interactions with the TYR444 and the N5 atom of the flavin adenine dinucleotide (FAD) unit of MAO-A, respectively. **SB5** adopts an 'L' type configuration in which the aryl thiosemicarbazone unit is accommodated by the facing FAD unit with a hydrogen bond of distance 2.15 Å surrounded by the aromatic cage of TYR444 and TYR407. The

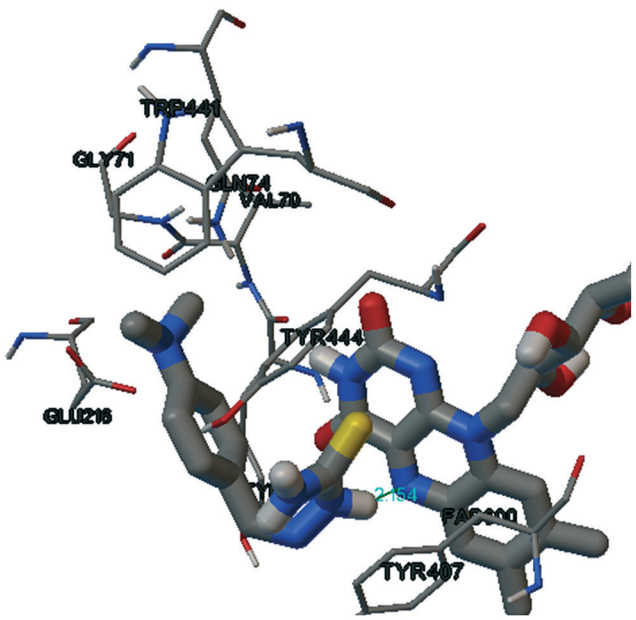

Fig. 5 **SB5** in the active site of MAO-A.

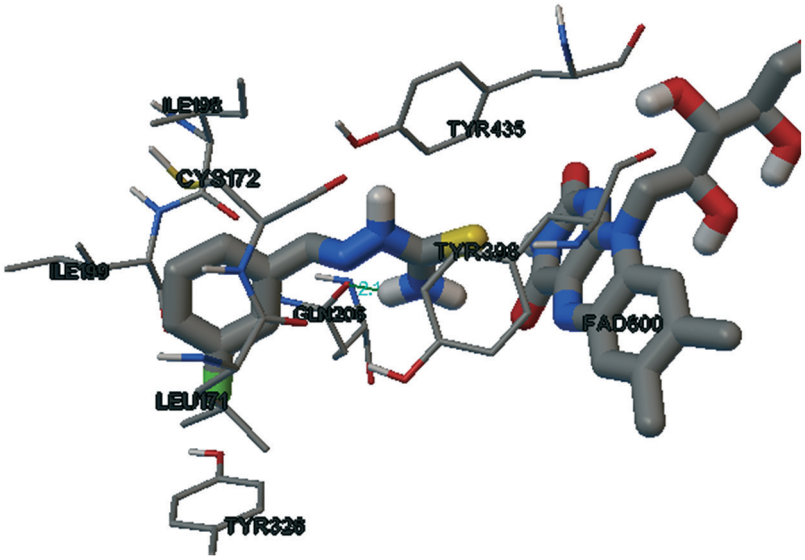

Fig. 6 **SB11** in the active site of MAO-B.

position and close proximity towards the FAD unit of **SB5** may enhance its binding energy towards MAO-A.

The binding mode of the potent MAO-B inhibitor **SB11** is shown in Fig. 6. The entrance cavity of MAO-B leading to the substrate cavity is hydrophobic in nature.[52] ILE199 and TYR326 are the side chains responsible for the separation and fusion between the entrance and substrate cavity, depending on the nature of the bound inhibitor.[53–56] The *meta* substituted fluorine of the phenyl system of **SB11** is efficiently accommodated in the entrance cavity of MAO-B. This lipophilic environment enhances the binding affinity of **SB11** towards the IBC of MAO-B. The terminal amino group of thiosemicarbazone shows significant hydrogen bonding with GLN206 and the electron rich thiocarbamoyl group of **SB11** surrounded by the aromatic cage of TYR398 and TYR435 nearer to the FAD unit.

Conclusions

To summarize our results, various aryl thiosemicarbazones with different electron donating and withdrawing environments were synthesized, characterized and evaluated for their MAO inhibitory and blood brain barrier permeation potential. The representative compounds **SB5** and **SB11** were potent for MAO-A and MAO-B, respectively, with a reversible and competitive mode of inhibition, having IC_{50} values of 1.82 ± 0.14 and 0.27 ± 0.015 μM, respectively. The results explicate that the nature and orientation of groups on the aryl system of the title scaffold can bestow a significant selectivity profile on both MAO-A and MAO-B. The SAR revealed that the presence of an electron donating bulky group produces good selectivity towards MAO, and at the same the time an electron withdrawing nitro group in the same position shifts the selectivity to MAO-B. The presence of a halogen at the *para* position of the phenyl ring has no impact on MAO inhibition, but the shifting of fluorine to the *meta* position dramatically results in good MAO-B inhibition with a high selectivity index. Compounds **SB5**, **SB7** and **SB11** show moderate inhibition against acetylcholinesterase with IC_{50} values of 35.35 ± 0.47, 15.61 ± 0.057 and 26.61 ± 0.338 μM, respectively. PAMPA studies revealed that the representative molecules are able to cross the blood–brain barrier, which is a pre-requisite of CNS drug design for the treatment of various neurodegenerative and psychiatric disorders. Molecular modelling studies identified that the presence of the imino nitrogen and terminal amino group of **SB5** contributed significant hydrogen bonding interactions with the TYR444 and N5 atom of the flavin adenine dinucleotide (FAD) unit of MAO-A, and the *m*-fluorine of the phenyl system of **SB11** was efficiently accommodated in the entrance cavity of the MAO-B. Also, the terminal amino group of thiosemicarbazone formed significant hydrogen bonding with GLN206 of MAO-B. This study has thus provided new insights into the SARs of various aryl thiosemicarbazone compounds towards MAO inhibition and could possibly afford new attractive and more promising multi-targeted ligands for the treatment of AD and PD.

Experimental

Chemistry

A mixture of thiosemicarbazide hydrochloride and substituted benzaldehyde in the presence of catalytic acetic acid was stirred for 3–4 hours. The resultant mixture was refluxed for 4–5 hours and poured onto crushed ice. The formed solid was washed with water until it was free from the acid, filtered and crystallized with ethanol. The following 13 phenyl substituted thiosemicarbazones (**SB1**–**SB13**) were obtained:

(2*E*)-2-Benzylidenehydrazine-1-carbothioamide (SB1). Yellowish white; yield: 76%; m.p.: 126–128 °C. ^{1}H NMR (400

MHz, $CDCl_3$) δ: 6.40 (s, 1H, NH_2), 7.23 (s, 1H, NH_2), 7.44–7.42 (m, 3H, J = 8 Hz, Ar–H), 7.66–7.64 (d, 2H, J = 8 Hz, Ar–H), 7.86 (s, 1H, –CH═N–), 9.60 (s, 1H, ═N–NH–C═S). ^{13}C-NMR (100 MHz, $CDCl_3$) δ: 182.6 (C═S), 142.8 (CH═N), 134.3 (Ar–C1), 131.0 (Ar–C4), 129.3 (Ar–C2 & Ar–C6), 128.6 (Ar–C3 & Ar–C5). ESI-MS (m/z): calculated-179.24, observed-361.23.

(2*E*)-2-[(4-Hydroxyphenyl)methylidene]hydrazine-1-carbothioamide (SB2). Pale yellow; yield: 63%; m.p.: 210–212 °C. ^{1}H NMR (400 MHz, $CDCl_3$) δ: 5.21 (s, IH, Ar–OH) 6.77, (s, 1H, NH_2), 6.94–6.92 (d, 2H, J = 8 Hz, Ar–H), 7.28 (s, 1H, NH_2), 7.66–7.64 (d, 2H, J = 8 Hz, Ar–H), 7.77 (s, 1H, –CH═N–), 9.56 (s, 1H, ═N–NH–C═S). ^{13}C-NMR (100 MHz, $CDCl_3$) δ: 181.3 (C═S), 160.2 (Ar–C4), 142.37 (CH═N), 130.3 (Ar–C2 & Ar–C6), 125.2 (Ar–C1), 118.2 (Ar–C3 & Ar–C5). ESI-MS (m/z): calculated-195.24, observed-195.23.

(2*E*)-2-[(4-Methoxyphenyl)methylidene]hydrazine-1-carbothioamide (SB3). Yellowish; yield: 78%; m.p.: 150–152 °C. ^{1}H NMR (400 MHz, $CDCl_3$) δ: 3.84 (s, 3H, OCH_3), 6.37 (s, 1H, NH_2), 6.92–6.90 (d, 2H, J = 8 Hz, Ar–H), 7.26 (s, 1H, NH_2), 7.60–7.58 (d, 2H, J = 8 Hz, Ar–H), 7.83 (s, 1H, –CH═N–), 9.66 (s, 1H, ═N–NH–C═S). ^{13}C-NMR (100 MHz, $CDCl_3$) δ: 181.4 (C═S), 161.9 (Ar–C4), 145.2 (CH═N), 129.8 (Ar–C2 & Ar–C6), 128.9 (Ar–C1), 119.3 (Ar–C3 & Ar–C5), 55.4 (OCH_3). ESI-MS (m/z): calculated-209.26, observed-209.25.

(2*E*)-2-[(4-Methylphenyl)methylidene]hydrazine-1-carbothioamide (SB4). White; yield: 82%; m.p.: 155–157 °C. ^{1}H NMR (400 MHz, $CDCl_3$) δ: 2.38 (s, 3H, CH_3), 6.46 (s, 1H, NH_2), 7.21–7.19 (d, 2H, J = 8 Hz, Ar–H), 7.26 (s, 1H, NH_2), 7.54–7.52 (d, 2H, J = 8 Hz, Ar–H), 7.88 (s, 1H, –CH═N–), 9.88 (s, 1H, ═N–NH–C═S). ^{13}C-NMR (100 MHz, $CDCl_3$) δ: 181.6 (C═S), 145.3 (CH═N), 142.1 (Ar–C4), 132.2 (Ar–C1), 131.7 (Ar–C2 & Ar–C6), 131.4 (Ar–C3 & Ar–C5), 21.6 (CH_3). ESI-MS (m/z): calculated-193.26, observed-193.25.

(2*E*)-2-{[4-(Dimethylamino)phenyl]methylidene}hydrazine-1-carbothioamide (SB5). Yellowish; yield: 81%; m.p.: 190–192 °C. ^{1}H NMR (400 MHz, $CDCl_3$) δ: 3.03 (s, 6H, $N(CH_3)_2$), 6.23 (s, 1H, NH_2), 6.68–6.66 (d, 2H, J = 12 Hz, Ar–H), 7.26 (s, 1H, NH_2), 7.52–7.49 (d, 2H, J = 12 Hz, Ar–H), 7.71 (s, 1H, –CH═N–), 9.18 (s, 1H, ═N–NH–C═S). ^{13}C-NMR (100 MHz, $CDCl_3$) δ: 181.7 (C═S), 151.8 (Ar–C4), 141.4 (CH–N), 132.0 (Ar–C2 & Ar–C6), 123.5 (Ar–C1), 114.4 (Ar–C3 & Ar–C5), 41.9 (N–$(CH_3)_2$). ESI-MS (m/z): calculated-222.30, observed-222.29.

(2*E*)-2-[(4-Ethylphenyl)methylidene]hydrazine-1-carbothioamide (SB6). White; yield: 84%; m.p.: 125–126 °C. ^{1}H NMR (400 MHz, $CDCl_3$) δ: 1.24–1.22 (t, 3H, J = 8 Hz, CH_3), 2.70–2.68 (q, 2H, J = 8 Hz, CH_2), 6.47 (s, 1H, NH_2), 7.24–7.22 (d, 2H, J = 8 Hz, Ar–H), 7.26 (s, 1H, NH_2), 7.57–7.55 (d, 2H, J = 8 Hz, Ar–H), 7.89 (s, 1H, –CH═N–), 9.92 (s, 1H, ═N–NH–C═S). ^{13}C-NMR (100 MHz, $CDCl_3$) δ: 181.2 (C═S), 145.99 (CH═N), 137.3 (Ar–C4), 130.5 (Ar–C1), 129.8 (Ar–C2 & Ar–C6), 128.8 (Ar–C3 & Ar–C5), 33.5 (CH_2), 14.8 (CH_3). ESI-MS (m/z): calculated-207.29, observed-207.00.

(2*E*)-2-[(4-Nitrophenyl)methylidene]hydrazine-1-carbothioamide (SB7). Turmeric yellow; yield: 82%; m.p.: 220–222 °C. ^{1}H NMR (400 MHz, $CDCl_3$) δ: 6.23 (s, 1H, NH_2), 6.68–6.66 (d, 2H, J = 8 Hz, Ar–H), 7.26 (s, 1H, NH_2), 7.52–7.49 (d, 2H, J = 12 Hz, Ar–H), 7.71 (s, 1H, –CH═N–), 9.20 (s, 1H, ═N–NH–C═S). ^{13}C-NMR (100 MHz, $CDCl_3$) δ: 183.9 (C═S), 150.2 (Ar–C4), 143.4 (CH═N), 136.9 (Ar–C1), 131.3 (Ar–C2 & Ar–C6), 124.5 (Ar–C3 & Ar–C5). ESI-MS (m/z): calculated-224.23, observed-224.22.

(2*E*)-2-[(4-Chlorophenyl)methylidene]hydrazine-1-carbothioamide (SB8). Pale white; yield: 83%; m.p.: 175–177 °C. ^{1}H NMR (400 MHz, $CDCl_3$) δ: 7.25 (s, 1H, NH_2), 7.40–7.38 (d, 2H, J = 8 Hz, Ar–H), 7.26 (s, 1H, NH_2), 7.59–7.57 (d, 2H, J = 12 Hz, Ar–H), 7.78 (s, 1H, –CH═N–), 9.33 (s, 1H, ═N–NH–C═S). ^{13}C-NMR (100 MHz, $CDCl_3$) δ: 184.3 (C═S), 142.9 (CH═N), 137.3 (Ar–C4), 131.3 (Ar–C1), 130.6 (Ar–C2 & Ar–C6), 130.5 (Ar–C3 & Ar–C5). ESI-MS (m/z): calculated-213.68, observed-213.67.

(2*E*)-2-[(4-Bromophenyl)methylidene]hydrazine-1-carbothioamide (SB9). White; yield: 85%; m.p.: 140–142 °C. ^{1}H NMR (400 MHz, $CDCl_3$) δ: 6.39 (s, 1H, NH_2), 7.26 (s, 1H, NH_2), 7.56–7.54 (d, 4H, J = 8 Hz, Ar–H), 7.76 (s, 1H, –CH═N–), 9.29 (s, 1H, ═N–NH–C═S). ^{13}C-NMR (100 MHz, $CDCl_3$) δ: 182.0 (C═S), 142.9 (CH═N), 131.2 (Ar–C1), 130.3 (Ar–C2 & Ar–C6), 130.2 (Ar–C3 & Ar–C5), 121.6 (Ar–C4).ESI-MS (m/z): calculated-258.13, observed-258.13.

(2*E*)-2-[(4-Fluorophenyl)methylidene]hydrazine-1-carbothioamide (SB10). White; yield: 82%; m.p.: 120–122 °C. ^{1}H NMR (400 MHz, $CDCl_3$) δ: 6.38 (s, 1H, NH_2), 7.40–7.38 (d, 2H, J = 8 Hz, Ar–H), 7.26 (s, 1H, NH_2), 7.59–7.57 (d, 2H, J = 12 Hz, Ar–H), 7.78 (s, 1H, –CH═N–), 9.33 (s, 1H, ═N–NH–C═S). ^{13}C-NMR (100 MHz, $CDCl_3$) δ: 180.6 (C═S), 160.3 (Ar–C4), 142.2 (CH═N), 131.3 (Ar–C1), 130.6 (Ar–C2 & Ar–C6), 125.6 (d, J_{C-F} = 62 Hz, Ar–C3 & Ar–C5). ESI-MS (m/z): calculated-197.23, observed-197.23.

(2*E*)-2-[(3-Fluorophenyl)methylidene]hydrazine-1-carbothioamide (SB11). Pinkish white; yield: 79%; m.p.: 155–157 °C. ^{1}H NMR (400 MHz, $CDCl_3$) δ: 6.39 (s, 1H, NH_2), 7.26 (s, 1H, NH_2), 7.56–7.54 (m, 4H, J = 8 Hz, Ar–H), 7.76 (s, 1H, –CH═N–), 9.29 (s, 1H, ═N–NH–C═S). ^{13}C-NMR (100 MHz, $CDCl_3$) δ: 182.2 (C═S), 166.2 (Ar–C3), 140.1 (CH═N), 136.6, (Ar–C5), 134.3 (Ar–C1), 125.3 (Ar–C6), 122.9 (d, J_{C-F} = 64 Hz, Ar–C4), 121.6 (d, J_{C-F} = 68 Hz, Ar–C2). ESI-MS (m/z): calculated-197.23, observed-197.23.

(2*E*)-2-[(2-Fluorophenyl)methylidene]hydrazine-1-carbothioamide (SB12). Yellowish grey; yield: 82%; m.p.: 121–123 °C. ^{1}H NMR (400 MHz, $CDCl_3$) δ: ^{1}H NMR (400 MHz, $CDCl_3$) δ: 6.38 (s, 1H, NH_2), 7.12–7.10 (m, 2H, J = 8 Hz, Ar–H), 7.26 (s, 1H, NH_2), 7.65–7.63 (m, 2H, J = 8 Hz, Ar–H), 7.85 (s, 1H, –CH═N–), 9.66 (s, 1H, ═N–NH–C═S). ^{13}C-NMR (100 MHz, $CDCl_3$) δ: 182.1 (C═S), 164.1 (Ar–C2), 143.6 (CH═N), 134.3, (d, J_{C-F} = 68 Hz, Ar–C4), 130.2 (Ar–C6), 125.2 (Ar–C5), 122.6 (Ar–C1), 121.5 (Ar–C3). ESI-MS (m/z): calculated-197.23, observed-197.22.

(2*E*)-2-{[4-(Trifluoromethyl)phenyl]methylidene}hydrazine-1-carbothioamide (SB13). Grey; yield: 79%; m.p.: 135–137 °C. ^{1}H NMR (400 MHz, $CDCl_3$) δ: ^{1}H NMR (400 MHz, $CDCl_3$) δ: 6.44 (s, 1H, NH_2), 7.11–7.09 (d, 2H, J = 8 Hz, Ar–H), 7.26 (s, 1H, NH_2), 7.37–7.35 (d, 2H, J = 12 Hz, Ar–H), 7.87 (s, 1H, –CH═N–), 9.83 (s, 1H, ═N–NH–C═S). ^{13}C-NMR (100 MHz, $CDCl_3$) δ: 181.4 (C═S), 160.3 (Ar–C4), 142.1 (CH═N), 138.4 (Ar–C1),

135.6 (Ar–C4), 129.2 (Ar–C2 & Ar–C6), 124.3 (q, J_{C-F} = 278 Hz, Ar–C3 & Ar–C5), 123.6 (CF_3). ESI-MS (*m*/*z*): calculated-247.24, observed-247.23.

Monoamine oxidase inhibition studies

Enzyme assays. Chemicals and enzymes were used as described previously. MAO activities were assayed by the continuous method using 0.06 mM kynuramine for MAO-A and 0.3 mM benzylamine for MAO-B as substrates, and reaction rates were expressed as absorbance change per min. The K_m values of kynuramine and benzylamine obtained in this study were 0.040 mM and 0.15 mM, respectively, and the substrate concentrations used were 1.5 × and 2.0 × K_m values, respectively.[57]

Analysis of inhibitory activities and enzyme kinetics. The inhibitions of MAO-A or MAO-B activities by the 13 compounds were primarily analyzed at a concentration of 10 μM. The IC_{50} values were then determined for 6 compounds showing more than 50% inhibitory activity, along with the reference compounds for reversible and irreversible inhibitors. Two potent compounds, **SB5** for MAO-A and **SB11** for MAO-B, were further investigated for time-dependent inhibition, kinetic studies for assessing the inhibition types, and K_i values of the compounds, as previously described.[58]

Analysis of reversibility of the inhibitors. Reversibility experiments for the potent inhibitors were performed using the dialysis method, including reference compounds for reversible and irreversible inhibitors, as previously described. The experiments were conducted using 3.6 μM **SB5** for MAO-A and 0.54 μM **SB11** for MAO-B in 100 mM sodium phosphate (pH 7.2) after preincubation for 30 min. Residual activities for undialyzed and dialyzed experiments were measured, and the relative activities for undialyzed (A_U) and dialyzed (A_D) experiments were calculated by comparing with each control without an inhibitor. The reversibility pattern was determined by comparing the relative A_U and A_D values.[59]

Acetylcholinesterase inhibition

AChE inhibitory activity was assayed using the method developed by Ellman *et al.*, with slight modifications. The reaction was assayed for 10 min at 412 nm using 0.2 U ml^{-1} of AChE (*Electrophorus electricus*, type VI-S, Sigma) in 0.5 ml reaction mixture of 50 mM sodium phosphate (pH 7.5), in the presence of 0.5 mM 5,5′-dithiobis(2-nitrobenzoic acid) (DTNB) and 0.5 mM acetylthiocholine iodide (ACTI). For the measurement of inhibitory activity, each inhibitor (and tacrine as a reference) was preincubated for 15 min with the enzyme prior to addition of DTNB and ACTI.[60]

Blood–brain barrier (BBB) assay

The 6 top ranked synthesized thiosemicarbazones and known commercial drugs were dissolved in DMSO at a final concentration of 5 mg mL^{-1}, followed by appropriate dilution with a 70 : 30 mixture of phosphate buffered saline solution and ethanol (PBS/EtOH) to give a final concentration of 25 μg mL^{-1}. The filter membrane in the donor microplate was coated with polar brain lipid (PBL) dissolved in dodecane (4 μg mL^{-1}, 20 mg mL^{-1}). A total of 200 μL of diluted solution and 300 μL of PBS/EtOH (70 : 30) were added to the donor and the acceptor wells, respectively. The donor filter plate was carefully placed on the acceptor plate, and the sandwich system was kept at 25 °C for 16 h. The donor plate was carefully removed, and the concentrations of the compounds and the commercial drugs in the acceptor, donor and reference wells were measured with a UV plate reader.[51]

Molecular docking

AutoDock 4.2 software was employed for molecular docking studies of the lead molecules.[61] Preparation Wizard of Maestro-8.4 (Schrodinger LLC) was used to prepare the protein. Crystallographic models 2BXR (hMAO-A) and 2BYB (hMAO-B) were downloaded from www.rcsb.org.[62] Ligands were prepared through the PRODRG webserver (http://davapc1.bioch.dundee.ac.uk/cgi-bin/prodrg).[63] Grid preparation was performed and the docking parameters were prepared on the basis of a reported method.[64]

Conflicts of interest

There are no conflicts of interest to declare.

Acknowledgements

This research was supported by the Basic Science Research Program through the National Research Foundation (NRF) of Korea, which is funded by the Ministry of Education (2017R1D1A3B03028559 granted to H. Kim).

References

1 K. F. Tripton, *Cell Biochem. Funct.*, 1986, **4**, 79–87.
2 R. R. Ramsay, *Curr. Pharm. Des.*, 2013, **19**, 2529–2539.
3 B. Kumar, Sheetal, A. K. Mantha and V. Kumar, *RSC Adv.*, 2016, **6**, 42660–42683.
4 S. Carradori, D. Secci, A. Bolasco, P. Chiment and M. D' Asceenzio, *Expert Opin. Ther. Pat.*, 2012, **22**, 909–939.
5 B. Mathew, J. Suresh, G. E. Mathew, S. A. Rasheed, J. K. Vilapurathu and P. Jayaraj, *Curr. Enzyme Inhib.*, 2015, **11**, 108–115.
6 M. B. Youdim and Y. S. Bakhle, *Br. J. Pharmacol.*, 2006, **147**, S287–S296.
7 M. B. Youdim, D. Edmondson and K. F. Tripton, *Nat. Rev. Neurosci.*, 2006, **7**, 295–309.
8 P. Riederer and T. Muller, *Expert Opin. Drug Metab. Toxicol.*, 2017, **13**, 233–240.
9 B. Mathew, S. Dev, M. Joy and G. E. Mathew, *ChemistrySelect*, 2017, **2**, 11645–11652.
10 C. Binda, E. M. Milczek, D. Bonivento, J. Wang, A. Mattevi and D. E. Edmondson, *Curr. Top. Med. Chem.*, 2011, **11**, 2788–2796.

11 L. Pisani, M. Catto, F. Leonetti, O. Nicolotti, A. Stefanachi, F. Campagna and A. Carotti, *Curr. Med. Chem.*, 2011, **18**, 4568–4587.
12 M. B. H. Youdim and M. B. H. Curr, *Alzheimers Res. Ther.*, 2006, **3**, 541–550.
13 S. Carradori and R. Silvestri, *J. Med. Chem.*, 2015, **85**, 6717–6732.
14 C. Binda, M. Li, F. Hubaìlek, N. Restelli, D. E. Edmondson and A. Mattevi, *Proc. Natl. Acad. Sci. U. S. A.*, 2003, **100**, 9750–9755.
15 M. B. Youdim and M. Weinstock, *NeuroToxicology*, 2004, **25**, 243–250.
16 K. Sieradzan, S. Channon, C. Ramponi, G. M. Stern, A. J. Lees and M. B. Youdim, *J. Clin. Psychopharmacol.*, 1995, **15**, 51S–59S.
17 B. Mathew, A. Haridas, J. Suresh, G. E. Mathew, G. Ucar and V. Jayaprakash, *Cent. Nerv. Syst. Agents Med. Chem.*, 2016, **16**, 120–136.
18 M. J. Matos, D. Vina, S. Vazque-Rodrigues, E. Uriarte and L. Santana, *Curr. Top. Med. Chem.*, 2012, **12**, 2210–2239.
19 B. Mathew, G. E. Mathew, J. P. Petzer and A. Petzer, *Comb. Chem. High Throughput Screening*, 2017, **20**, 522–532.
20 S. Kasayuki Uda, *J. Heterocycl. Chem.*, 1979, **16**, 1273–1278.
21 K. N. Zelenin, O. R. Kuzenetsova, V. V. Alekseyev, P. B. Terentyev and V. V. Ovacharenko, *Tetrahedron*, 1993, **49**, 1257–1270.
22 Y. Yu, D. S. Kalinowski, Z. Kovacevic, A. R. Siafakas, P. J. Jansson and C. Stefani, *et al.*, *J. Med. Chem.*, 2009, **52**, 5271–5294.
23 S. Tripathi, B. R. Pandaey, J. P. Barthwal, K. Kishor and K. P. Bhargava, *Res. Commun. Chem. Pathol. Pharmacol.*, 1978, **22**, 291–300.
24 D. K. Agarwal and B. R. Pandaey, *Res. Commun. Chem. Pathol. Pharmacol.*, 1979, **26**, 525–531.
25 F. Chimenti, E. Maccioni, D. Secci, A. Bolasco, A. Chimenti and A. Granese, *et al.*, *J. Med. Chem.*, 2008, **51**, 4874–4880.
26 R. K. P. Tripathi, O. Goshain and S. R. Ayyannan, *ChemMedChem*, 2013, **8**, 462–474.
27 R. K. P. Tripathi, G. K. Rai and S. R. Ayyannan, *ChemMedChem*, 2016, **11**, 1145–1160.
28 R. K. P. Tripathi, M. Sasi, S. K. Gupta, S. Krishnamurthy, S. R. Ayyannan and J. Enzyme Inhib, *Med. Chem.*, 2018, **33**, 37–57.
29 R. Pignatello, S. Mazzone, F. Castelli, P. Mazzone, G. Raciti and G. Mazzone, *Pharmazie*, 1994, **49**, 272–276.
30 N. Gokhan, A. Yesilada, G. Ucar, K. Erol and A. A. Bilgin, *Arch. Pharm.*, 2003, **336**, 362–371.
31 G. Ucar, N. Gokhan, A. Yesilada and A. A. Bilgin, *Neurosci. Lett.*, 2005, **382**, 327–331.
32 S. Yabanoglu, G. Ucar, S. Gokhan, U. Salgin, A. Yesilada and A. A. Bilgin, *J. Neural Transm.*, 2007, **114**, 769–773.
33 D. Secci, S. Carradori, A. Bolasco, B. Bizzarri, M. D'Ascenzio and E. Maccioni, *Curr. Top. Med. Chem.*, 2012, **12**, 2240–2257.
34 B. Mathew, J. Suresh, S. Anbazhagan and G. E. Mathew, *Cent. Nerv. Syst. Agents Med. Chem.*, 2013, **13**, 195–206.
35 B. Mathew, J. Suresh, M. J. Ahasan, G. E. Mathew, D. Usman and P. N. Subramanyan, *et al.*, *Infect. Disord.: Drug Targets*, 2015, **15**, 76–88.
36 D. Vina, M. J. Matos, M. Yanez, L. Santana and E. Uriarte, *Med. Chem. Commun.*, 2012, **3**, 213–218.
37 W. J. Geldenhuys, K. S. Ko, H. Stinneft and C. J. Van der Schyf, *Med. Chem. Commun.*, 2011, **2**, 1099–1103.
38 N. A. Soares, M. A. Almeida, C. Marins-Goulart, O. A. Chaves, A. Echevarria and M. C. C. de Oliveria, *Bioorg. Med. Chem. Lett.*, 2017, **27**, 3546–3550.
39 G. R. Subhashree, J. Haribabu, S. Saranya, P. Yuvaraj, D. Krishnan and R. Karvenbu, *et al.*, *J. Mol. Struct.*, 2017, **1145**, 160–169.
40 P. Liciano, C. B. Moraes, L. M. Alcantara, C. H. Franco, B. Pascoalino and L. H. Freitas-Junior, *et al.*, *Eur. J. Med. Chem.*, 2018, **146**, 423–434.
41 R. Sasidharan, S. C. Baek, S. L. Manju, H. Kim and B. Mathew, *Biomed. Pharmacother.*, 2018, **106**, 8–13.
42 B. Mathew, G. Ucar, S. Y. Ciftci, I. Baysal, J. Suresh, G. E. Mathew, J. K. Vilapurathu, N. A. Moosa, N. Pullarottil, L. Viswam, A. Haridas and F. Fathima, *Lett. Org. Chem.*, 2015, **12**, 605–613.
43 B. Mathew, G. E. Mathew, G. Ucar, I. Baysal, J. Suresh, J. K. Vilapurathu, A. Prakasan, J. K. Suresh and A. Thomas, *Bioorg. Chem.*, 2015, **62**, 22–29.
44 B. Mathew, G. E. Mathew, G. Ucar, I. Baysal, J. Suresh, S. Mathew, A. Haridas and V. Jayaprakash, *Chem. Biodiversity*, 2016, **13**, 1046–1052.
45 B. Mathew, G. Ucar, G. E. Mathew, S. Mathew, P. K. Purapurath, F. Moolayil, S. Mohan and S. V. Gupta, *ChemMedChem*, 2016, **11**, 2649–2655.
46 B. Mathew, A. Haridas, G. Ucar, I. Baysal, A. A. Adeniyi, M. E. S. Soliman, M. Joy, G. E. Mathew, B. Lakshmanan and V. Jayaprakash, *Int. J. Biol. Macromol.*, 2016, **91**, 680–695.
47 B. Mathew, A. Haridas, G. Ucar, I. Baysal, M. Joy, G. E. Mathew, B. Lakshmanan and V. Jayaprakash, *ChemMedChem*, 2016, **11**, 1161–1171.
48 R. Sasidharan, S. L. Manju, G. Ucar, I. Baysal and B. Mathew, *Arch. Pharm.*, 2016, **349**, 627–637.
49 B. Mathew, G. E. Mathew, G. Ucar, G. E. Mathew, E. K. Nafna, K. L. Lohidakshan and J. Suresh, *Int. J. Biol. Macromol.*, 2017, **104**, 1321–1329.
50 B. Mathew, G. Ucar, C. Raphael, G. E. Mathew, M. Joy, K. E. Machaba and M. E. S. Soliman, *ChemistrySelect*, 2017, **2**, 11113–11119.
51 L. Di, E. H. Kerns, K. Fan, O. J. McConnell and G. T. Carter, *Eur. J. Med. Chem.*, 2003, **38**, 223–232.
52 B. Mathew, A. A. Adeniyi, S. Dev, M. Joy, G. Ucar, G. E. Mathew, A. S. Pillay and M. E. S. Soliman, *J. Phys. Chem. B*, 2017, **121**, 1186–1203.
53 L. Novaroli, A. Daina, E. Favre, J. Bravo, A. Carotti and F. Leonetti, *et al.*, *J. Med. Chem.*, 2006, **49**, 6264–6272.
54 L. Legoabe, J. Kruger, A. Petzer, J. J. Bergh and J. P. Petzer, *Eur. J. Med. Chem.*, 2011, **46**, 5162–5174.
55 S. J. Lan, L. F. Pan, S. S. Xie, X. B. Wang and L. Y. Kong, *Med. Chem. Commun.*, 2015, **6**, 592–600.

56 S. J. Lan, T. Zang, Y. Liu, Y. Zahng, J. W. Hou and S. S. Xie, *et al.*, *Med. Chem. Commun.*, 2017, **8**, 471–478.
57 S. C. Baek, H. W. Lee, H. W. Ryu, M. G. Kang, D. Park and S. H. Kim, *Bioorg. Med. Chem. Lett.*, 2018, **28**, 584–588.
58 J. Suresh, S. C. Baek, S. P. Ramakrishnan, H. Kim and B. Mathew, *Int. J. Biol. Macromol.*, 2018, **108**, 660–664.
59 H. W. Lee, H. Choi, S. J. Nam, W. Fenical and H. Kim, *J. Microbiol. Biotechnol.*, 2017, **27**, 785–790.
60 G. L. Ellman, K. D. Courtney, V. Andres Jr. and R. M. Feather-Stone, *Biochem. Pharmacol.*, 1961, **7**, 88–95.
61 G. M. Morris, R. Huey, W. Lindstrom, M. F. Sanner, R. K. Belew, D. S. Goodsell and A. J. Olson, *J. Comput. Chem.*, 2009, **30**, 2785–2791.
62 L. De Colibus, M. Li, C. Binda, A. Lustig, D. E. Edmondson and A. Mattevi, *Proc. Natl. Acad. Sci. U. S. A.*, 2005, **102**(36), 12684–12689.
63 A. W. Schuttelkopf and D. M. van Aalten, *Acta Crystallogr., Sect. D: Biol. Crystallogr.*, 2004, **60**, 1355–1363.
64 B. Mathew, J. Suresh, S. Anbazhagan and S. Dev, *Biomed. Aging Pathol.*, 2014, **4**, 297–301.